Available online at www.sciencedirect.com

ScienceDirect

Physics Procedia 12 (2011) 76–81

Physics Procedia

LiM 2011

Optimization of the Energy Deposition in Glasses with Temporally-Shaped Femtosecond Laser Pulses

C. Mauclair[a,*], K. Mishchik[a], A. Mermillod-Blondin[b], A. Rosenfeld[b], I. V. Hertel[b], E. Audouard[a], R. Stoian[a]

[a]*Laboratoire Hubert Curien, Université de Lyon, Université J. Monnet, Saint-Etienne, France*
[b]*Max-Born-Institut, Berlin, Germany*

Abstract

Bulk machining of glasses with femtosecond laser pulses enables the fabrication of embedded optical functions. Due to the nonlinear character of the laser-matter interaction, structural modifications can occur within the focal region. To reach a full control of the process, ways of controlling the deposition of the laser energy inside the material have to be unveiled. From static and time-resolved pictures of bulk-excitation of a-SiO_2 and borosilicate glass, we show that particular laser temporal shapes such as picosecond sequences can better confine the energy deposition than the femtosecond sequence by reducing the propagation artifacts.

Keywords: Ultrafast laser; Waveguide writing; Pump-probe; Temporal shaping

1. Motivation / State of the Art

Ultrafast laser processing of bulk transparent materials is an efficient technique with a strong potential in integrated optics and lab-on-chip applications. For the last decade, researchers have demonstrated its potential with the fabrication of more and more complex photonic devices in the volume of transparent materials [1]. Micrometer-sized matrix modification can be obtained due to the highly non linear character of the interaction between the infrared ultrashort pulses and the transparent material. In particular, the local optical properties are affected by the irradiation, resulting in local variations of birefringence, absorption and refractive index [2]. Consequently, optical components can be photowritten in three dimensions by simple translation of one or several laser spots in the bulk of the sample [3, 4].

However, the process can highly depend on linear and nonlinear effects that can affect the propagation of the laser pulse to the focal region and thus, the success of the energy deposition in a sufficiently confined manner. With the aim of reaching a better control of the process, it is interesting to compare the influence of the laser pulse shape to find an optimal temporal sequence leading to a reduced volume of efficient excitation. We demonstrate here that

* Corresponding author. Tel.: +33 4 77 91 58 02; Fax: +33 4 77 91 57 81.
E-mail address: cyril.mauclair@univ-st-etienne.fr

doi:10.1016/j.phpro.2011.03.108

particular laser temporal shapes such as picosecond sequences can better confine the energy deposition by reducing the propagation artifacts in the bulk both a-SiO_2 and borosilicate glasses. The success of the laser energy coupling is evaluated from time-resolved microscopy pictures of the irradiated area where the transient electronic plasma as well as the subsequent pressure wave are observed.

2. Experimental

The experimental set up is based on a pump-probe technique [5,6] and is depicted on Figure1. The laser source is an ultrafast laser system delivering 160 fs pulses (full width half maximum FWHM) at 800 nm. The laser beam is divided into two parts, one being used to excite the material, while the second is employed to probe the irradiation volume. Before reaching the irradiated sample, the excitation beam goes through a temporal shaping apparatus allowing for tailoring of the pulse temporal profile. The probe beam is spatially magnified, frequency doubled, and used to image the excitation region perpendicularly to the excitation beam propagation axis, thus providing microscopic images with a subpicosecond time resolution.

A microscope objective (numerical aperture NA = 0.45) focuses the pump beam into the bulk of the sample, which are polished parallelepipeds of 3 × 20 × 10 mm of fused silica glass and borosilcate glass (BK7). The focal plane is adjusted at a depth of 200 µm in conditions of low wavefront distortions due to the air-glass interface. The blue probe beam enters the illumination path of a modified phase contrast microscope (Olympus BX41). The final picture is recorded with the help of an intensifying CCD camera. The transient electronic density N_c is estimated from the absorption map delivered by the 400nm probe following a Drude model under a few assumptions [6]. In the following we use the normalized electronic density N_c/N_{cr}, N_{cr} being the critical density at 400nm.

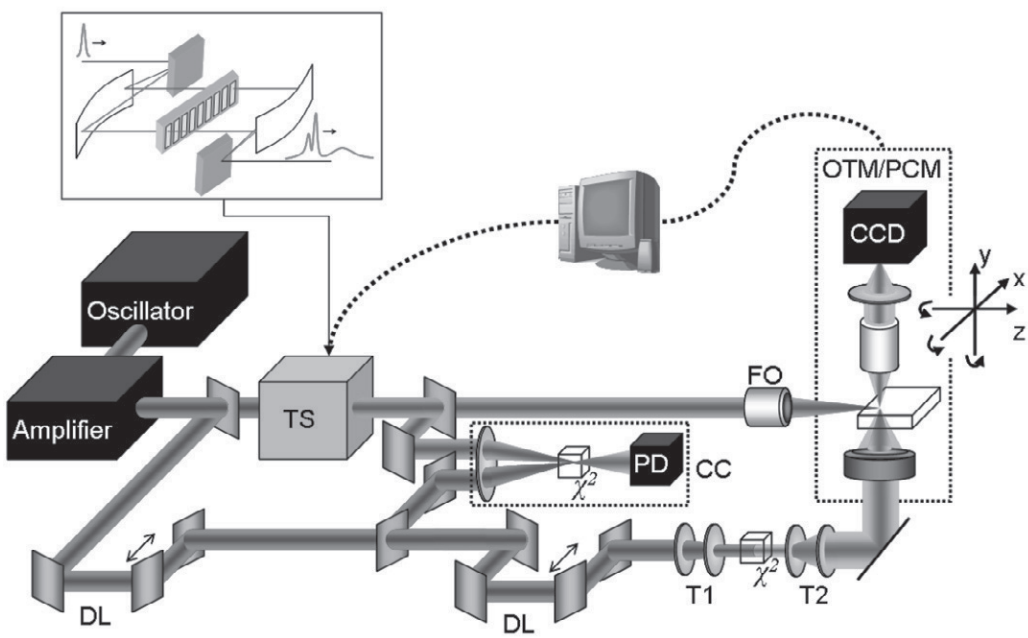

Figure 1. Experimental set up. TS: temporal shaper illustrated in the top inset. FO: focusing objective. OTM-PCM: Optical transmission and phase contrast microscopy χ^2 : Frequency doubling crystal. PD: Photodiode. CC: Cross-correlation apparatus. DL: delay line. T1, T2: Telescopes.

3. Results and discussion

3.1. Femtosecond and picosecond irradiation

The differences between femtosecond and picosecond irradiations of bulk dielectric materials were already investigated from their respective permanent modifications [7-9]. In fused silica, a stronger energy confinement leading to more contrasted and compact bulk modifications in the case of picosecond pulses was reported and verified by NLSE simulations [8]. Here, these observations are correlated with the transient free electronic density deduced from time-resolved microscopy images.

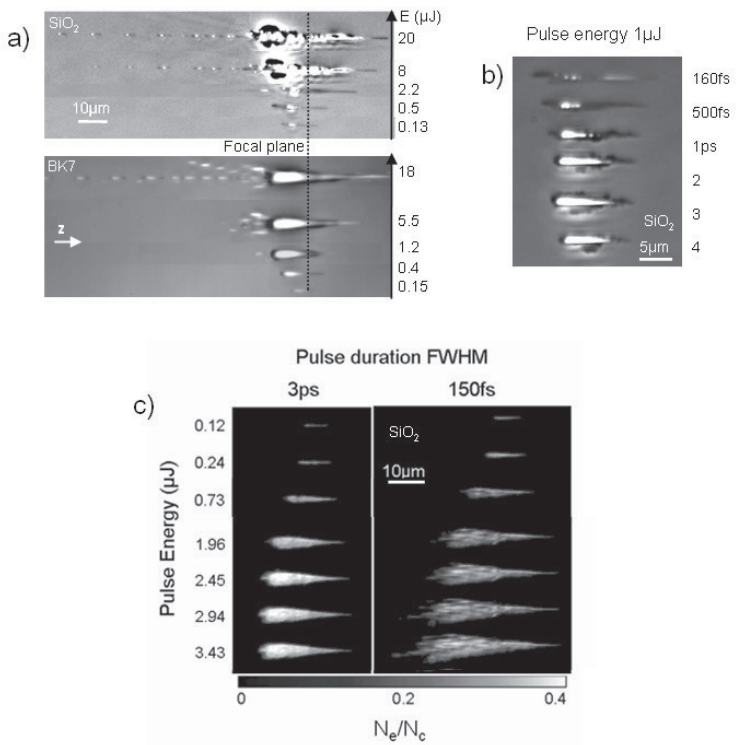

Figure 2 Comparison of single femtosecond and picosecond irradiation from permanent and transient modifications in fused silica and BK7 glass. a). PCM pictures of single pulse irradiation effects in fused silica and BK7 glass at different pulse energies (E). The laser propagates along z. For both glasses, the permanently modified volume extends around the focal plane increasingly with the pulse energy. b) Effect of the pulse duration in fused silica. c) Intensity dependence of the transient electronic density N_e normalized to N_{cr} for femtosecond and picosecond pulse. The N_e/N_{cr} mapping is calculated from optical transmission microscopy pictures.

Employing the described experimental set-up, fused silica and BK7 glass samples were irradiated with single femtosecond and picosecond optical pulses. The corresponding permanent micrometric bulk modifications are pictured using the phase contrast microscope yielding the images in Figure 2 a) and b). As noticeable from Figure 2 a), a femtosecond pulse generates a modified volume around the focal plane. This volume extends with the augmentation of the pulse energy. We underline here the presence of very regular dots preceding the focal point at sufficiently high energetic dose, whose position corresponds to the fluence peaks of the focal volume [10]. Figure 2 b) illustrates the effect of longer pulse durations in fused silica at constant pulse energy. It is observable from these permanent modifications that the laser-induced change occupies a smaller volume for longer pulses.

Using the 400nm probe, we realized the side-picturing of the transient electronic plasma in fused silica at the delay of maximum absorption for single femtosecond irradiation sequences (150fs FWHM) and single picosecond sequences (3ps FWHM). In order to compare the mapping of energy deposition for these two exposures, the

investigations were conducted for different pulse energy. The corresponding experimental data is presented in Figure 2 c), showing noticeable differences in the laser-induced free electronic cloud between the femtosecond and the picosecond irradiations. More precisely, in the femtosecond case, an increase of the pulse energy augments the affected volume with no increase of the electronic density. In the picosecond case, the affected volume tends to saturate for higher energy while the free electronic density is increased. The 2D-mapping of the electronic density along the laser propagation axis is the main interest of these experimental results. When averaging the electronic density over the plasma in the two cases, the two following observations arise.

In the femtosecond case, the averaged electronic density N_e/N_{cr} remains constant over the entire cloud despite of the pulse energy except on a small area corresponding to the permanent white void where N_e/N_{cr} is slightly higher as already observed in [5]. While the volume occupied by the electronic cloud incessantly increases (see Figure 2 c) right), its density remains constant. Reasons for this behavior are linked with the efficient plasma generation that occurs soon in the ultrashort pulse propagation. Note that the starting point of the plasma for femtosecond pulses is always positioned before the picosecond irradiation on the z-axis (Figure 2 c)). This plasma generation extents further as well. The optical properties of the free carrier cloud are dominated by an increased absorption and a lower refractive index [6]. The latter has a defocusing effect on the laser pulse. Thus, the region of main beam concentration is pushed further as the beam propagates and looses intensity due to the plasma absorption. Consequently, the zone of interaction is elongated with a quasi-constant electronic density.

On the contrary, picosecond sequences permit an increase of the electronic density with the pulse energy mainly in the left part of the plasma (see Figure 2 c) left). The picosecond envelope induces a retarded, low density, and spatially modulated plasma. This creates a smaller negative shift for the incoming energy and less defocusing, helping thus to concentrate the energy. Additionally, the nonlinearity of excitation diminishes, allowing efficient absorption only in a restricted region. These time-resolved experimental results evidence in details the wide difference of energy deposition between femtosecond and picosecond pulses above the modification threshold from 2D-mapping of N_{cr}. This was already predicted by numerical calculations involving the non linear Schrödinger equation [8]. Experiments were also carried out in borosilicate glass sample (BK7) with similar results regarding the better energy confinement in the case of longer pulses.

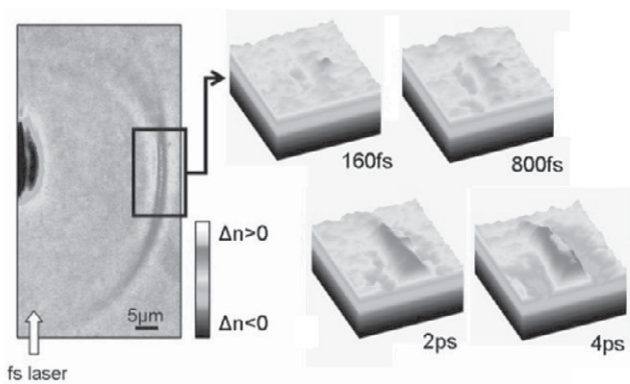

Figure 3: Pressure wave picturing from PCM images for various pulse duration in fused silica at constant pulse energy. (4.3 µJ, NA= 0.45)

3.2. Pressure wave as an energy transfer indicator

As the experimental set up allows for time resolved phase contrast picturing of the irradiated volume, minute variation of material densities are detectable on an ultrafast time-scale. Usually, upon energy relaxation, the temperature increase induces a corresponding pressure increase which relaxes via thermal expansion and shock generation. The subsequent generation of a traveling pressure wave [5] is readily observable under PCM after ~1ns.

Figure 3 shows the qualitative amplitude of the generated pressure wave for various pulse durations in fused silica in the same high energetic thermodynamic regime. As already reported [11], the pressure wave has a spherical shape. The refractive index variation associated with the traveling wave is supposed small enough to remain within

the linear response of the PCM measurement [12] permitting the comparison of their amplitude. The general observation of a stronger pressure wave in the case of picosecond pulse sequence has already been made [11], however the present experimental set up allow to precisely find the optimal pulse length to obtain the largest pressure wave amplitude (here 8 ps). Remarkably, the launching moment is identical for all the pulse durations involved here, denoting a similar energy coupling mechanism differing mostly in its efficiency and not in its chronology. In agreement with the results presented in the previous section on the transient electronic densities versus the pulse duration, the picosecond sequence is characterized by an enhanced energy confinement leading to a stronger pressure wave.

3.3. Chronology of the energy deposition for femtosecond and picosecond irradiations:

Taking advantage of the possibility offered by the set-up to temporally shape the excitation pulse, we carried time-resolved investigations for femtosecond and picosecond (3ps FWHM) pulse irradiations in fused silica. Each of the irradiation sequences carried 6 µJ to the bulk of the material. Again the free electronic density map was calculated following a Drude model from the 2D absorption maps delivered by the probe illuminating the sample. Figure 4 presents an overview of the corresponding results. On the left column, the two-dimensional map of the transient electronic cloud is represented for the three irradiation sequences showing a larger volume of interaction for the femtosecond pulse with a lens dense cloud. For the picosecond sequence however, the electronic gas is more confined and denser. On the right column, the maximum electronic density (N_e) normalized to the critical density (N_{cr}) at 800 nm is plotted versus time for the three pulse temporal shapes. We first remark the rather low free carrier density after 4 ps associated with the femtosecond pulse. Before that, however, the electronic density experiences a peak to the passage of the ultrashort pulse. This relatively high density quickly decreases as propagation non linearity spreads out the energy delivery.

On the contrary, the reduced amount of plasma defocusing for picosecond sequence [6] allows for more confined energy deposition where the major part of the pulse interacts with a free electronic plasma. This renders possible efficient energy absorption through inverse bremsstrahlung, augmenting the electrons kinetic energy along with the avalanche efficiency. A long-lasting free electronic density is obtained.

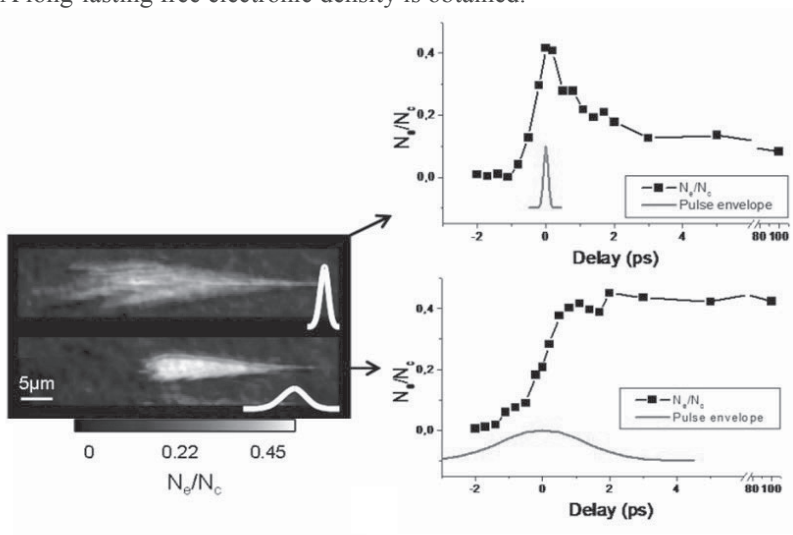

Figure 4. Calculated transient electronic density for single irradiation with (top) a 150 fs pulse and (middle) a 3 ps pulse. Each irradiation sequence carries 6 µJ. Left column: example of the Ne/Nc 2D map corresponding to the delay of maximum free carrier generation. Right column: temporal evolution of the maximum Ne/Nc with indication of the irradiation envelope. Laser comes from left.

In summary, from the transient electronic plasma densities as well as the amplitude of the laser induced pressure wave, we experimentally showed that temporal tailoring of ultrashort pulses can improve the efficiency of energy coupling to the matrix for bulk machining of transparent materials in an optimal manner.

References

[1] K. Itoh, W. Watanabe, S. Nolte, and C. Schaffer: Ultrafast Processes for Bulk Modification of Transparent Materials. In: MRS Bull, 31, (2006) 620–5
[2] E. Bricchi, B. G. Klappauf, and P. G. Kazansky: Form birefringence and negative index change created by femtosecond direct writing in transparent materials. In: Opt. Lett., 29, (2004) 119–21
[3] S. Nolte, M. Will, J. Burghoff and A. Tuennermann: Femtosecond waveguide writing: a new avenue to three-dimensional integrated optics. In: Appl. Phys. A, 77, (2003) 109-11
[4] C. Mauclair et al. : Dynamic ultrafast laser spatial tailoring for parallel micromachining of photonic devices in transparent materials. In: Opt. Express 17, (2009) 3531-42
[5] A. Mermillod-Blondin et al. : Dynamics of femtosecond laser induced voidlike structures in fused silica. In: Appl. Phys. Lett. 94, (2009) 041911
[6] C. Mauclair, Spatio-temporal ultrafast laser tailoring for bulk functionalization of transparent materials. Ph.D. Thesis Freie Universitat Berlin - Université J. Monnet Saint-Etienne (2010)
[7] B. C. Stuart, M. D. Feit, S. Herman, A. M. Rubenchik, B. W. Shore, and M. D. Perry : Optical ablation by high-power short-pulse lasers. J. Opt. Soc. Am. B 13(2):459–468 (1996)
[8] I. M. Burakov et al. : Spatial distribution of refractive index variations induced in bulk fused silica by single ultrashort and short laser pulses. J. Appl. Phys. 101(4):043506–7 (2007)
[9] A. Mermillod-Blondin et al. : Size correction in ultrafast laser processing of fused silica by temporal pulse shaping. Appl. Phys. Lett. 93, (2008) 021921-3
[10] C. Mauclair et al.: Single-pulse ultrafast laser imprinting of axial dot arrays in bulk glasses. Opt. Lett. 36, 325-327 (2011)
[11] A. Horn, E.W. Kreutz, and R. Poprawe. Ultrafast time-resolved photography of femtosecond laser induced modifications in BK7 glass and fused silica. Appl. Phys. A 79(4):923–925 (2004)
[12] T. Noda and S. Kawata. Separation of phase and absorption images in phase-contrast microscopy. J. Opt. Soc. Am. A 9(6):924–931 (1992)